

# DIELECTRIC BRAGG ACCELERATOR

A. Mizrahi, L. Schächter, Electrical Engineering Department, Technion, Haifa 32000, Israel

R. L. Byer, Department of Applied Physics, Stanford University – MC4085, Stanford, CA 94305, USA

R. H. Siemann, SLAC, MS-7, Stanford University, P.O. Box 4349, Stanford, CA 94309, USA

## Abstract

It is demonstrated that a planar Bragg reflection waveguide consisting of a series of dielectric layers may form an acceleration structure. It is shown that an interaction impedance per wavelength of over  $100\Omega$  is feasible with existing materials, Silica ( $\epsilon = 2.1$ ) and Zirconia ( $\epsilon = 4$ ), and if materials of high dielectric coefficient become available in the future, they may facilitate an interaction impedance per wavelength closer to  $500\Omega$ .

## 1 INTRODUCTION

Indications that solid-state lasers will reach wall-plug to light efficiencies of 30% or more make a laser-driven vacuum-accelerator increasingly appealing. Since at the wavelength of relevant lasers, dielectrics may sustain a significantly higher electric field and transmit power with reduced loss comparing to metals, the basic assumption is that laser accelerator structures will be made of dielectrics. Closed optical structures and near-field accelerators with dimensions comparable to the wavelength are both being considered. Examples of these two are: a) the LEAP [1] crossed laser beam accelerator where the interaction between the crossed laser beams and the particles is limited by slits to satisfy the Lawson-Woodward theorem [2, 3], and b) the *photonic band-gap* (PBG) concept where a laser pulse is guided in a dielectric structure with a vacuum tunnel bored in its center [4]. Lithography, which would result in planar structures, and optical fiber drawing are manufacturing techniques that seem well suited for laser driven structures that have typical dimensions of a few microns.

Motivated by the low-loss Bragg dielectric *planar* mirrors used in high-power lasers, it is suggested to harness this concept in order to confine the laser-field in an optical acceleration structure. Its essence is to form a hollow dielectric waveguide consisting of an almost perfect reflector made of a planar array of quarter-wavelength dielectric layers. In the transverse direction the geometry is similar to that of a dielectric mirror, however, its characteristics are slightly different since the wave number has a significant component ( $k = \omega/c$ ) *parallel* to the dielectric surfaces, whereas in the case of a high-power laser mirror, the wave impinges *perpendicularly*.

## 2 DESCRIPTION OF THE SYSTEM

Consider a planar symmetric dielectric waveguide ( $\partial/\partial y = 0$ ), as illustrated in Fig. 1, which has a vacuum inner layer of width  $2D_{\text{int}}$  and surrounding periodic layers made of two lossless materials  $\epsilon^{\text{I}}$ ,  $\epsilon^{\text{II}}$ , the first layer

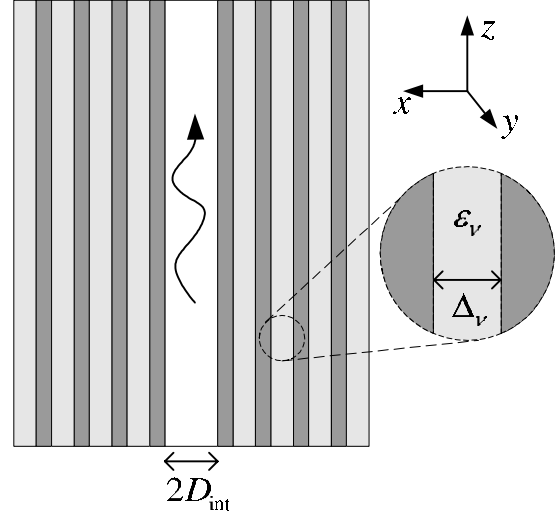


Figure 1: Planar dielectric waveguide.

having a relative dielectric coefficient  $\epsilon^{\text{I}}$ . Each layer has a thickness  $\Delta_\nu$  and a dielectric coefficient  $\epsilon_\nu$ . Assuming a steady-state regime ( $e^{j\omega t}$ ) we focus on a mode having a phase velocity equal to the speed of light, or explicitly in the vacuum layer the electromagnetic field reads,

$$\begin{aligned} E_z &= E_0 e^{-j\frac{\omega}{c}z} \\ E_x &= j\frac{\omega}{c}x E_0 e^{-j\frac{\omega}{c}z} \\ H_y &= \frac{j}{\eta_0} \frac{\omega}{c} x E_0 e^{-j\frac{\omega}{c}z} \end{aligned} \quad (1)$$

and the field components within some dielectric layer  $\nu$  are

$$\begin{aligned} E_z &= [A_\nu e^{-jk_\nu x} + B_\nu e^{+jk_\nu x}] e^{-j\frac{\omega}{c}z} \\ E_x &= \frac{-1}{\sqrt{\epsilon_\nu - 1}} [A_\nu e^{-jk_\nu x} - B_\nu e^{+jk_\nu x}] e^{-j\frac{\omega}{c}z} \\ H_y &= \frac{-1}{Z_\nu} [A_\nu e^{-jk_\nu x} - B_\nu e^{+jk_\nu x}] e^{-j\frac{\omega}{c}z} \end{aligned} \quad (2)$$

wherein

$$Z_\nu \triangleq \eta_0 \sqrt{\epsilon_\nu - 1} / \epsilon_\nu \quad (3)$$

is the transverse wave impedance and

$$k_\nu \triangleq \frac{\omega}{c} \sqrt{\epsilon_\nu - 1} \quad (4)$$

is the transverse wavenumber. Imposing the continuity of  $E_z$  and  $H_y$  at the interfaces between the dielectric layers, a plane-wave matrix formulation is obtained. Given the geometry and the dielectric coefficients of a waveguide that

supports the mode (1), the amplitudes in the second layer are dependent only on the vacuum fields. Imposing the continuity of the fields at the second boundary, we get that the amplitudes in the second layer depend only on the first and so forth, so that the amplitudes are determined from inside out.

### 3 FIELD CONFINEMENT

Analysis of the transverse propagation in the  $x$  direction is performed similarly to [5]. Assuming an infinite periodic structure, Floquet theorem leads to an eigen-value problem for the possible modes, and maximum attenuation per unit cell is seen to be achieved for the case of quarter-wavelength width layers. According to (4), each layer width should be  $\lambda/(4\sqrt{\epsilon-1})$ , and an exponential decay is obtained. The attenuation in one period is given by the ratio of the lower to higher wave impedances of the two dielectric layers. In case of a plane wave impinging perpendicularly upon a planar interface, the impedance is  $Z = \eta_0/\sqrt{\epsilon}$ , whereas if the wave has a phase velocity  $c$  in the  $z$  direction then the wave impedance is (3), which clearly has a maximum for  $\epsilon = 2$ .

The above description of the confinement process, is of an *infinite* and ideal Bragg reflector. In case of a *finite* structure imposed by the vacuum tunnel, the design constraints on the first layer are different. The first layer, whose amplitudes are completely determined by  $D_{\text{int}}/\lambda$  and  $\epsilon^{\text{I}}$ , should be of such width that at the interface with the next layer, the perfect reflection condition is met. It may be conceived as a matching layer between the vacuum region to the subsequent periodic structure, as it rotates the amplitude vector dictated by the vacuum mode, to overlap the eigen-vector of the periodic structure. Confinement entails vanishing *real* part of the transverse component of the complex Poynting vector, meaning that in each dielectric layer there is a standing wave. Taking  $E_0$  to be real without loss of generality, we get  $A_\nu = B_\nu^*$ . It is therefore evident that for the structure to truly support the mode, there must be an infinite number of layers, otherwise energy would "escape" and there would be no confinement. In a practical structure, the number of layers should be sufficient so that the outward power flow is negligible.

Fig. 2 illustrates a typical spatial distribution of the longitudinal electric field as well as the total electric field for a structure made of Silica ( $\epsilon^{\text{I}} = 2.1$ ) and Zirconia ( $\epsilon^{\text{II}} = 4$ ), and  $D_{\text{int}} = 0.3\lambda$ . It shows that  $E_z$  is uniform in the vacuum layer while oscillating and decaying exponentially in the Bragg layers. Another feature is that  $E_z$  vanishes and achieves a maximum alternately at the discontinuities, which can be proved to be mathematically equivalent to the quarter-wavelength condition. Accordingly, the transverse electric field  $E_x$ , derived from  $E_z$  with respect to  $x$ , is maximal and discontinuous whenever  $E_z$  is zero, and zero whenever  $E_z$  peaks. The total electric field in turn undergoes a discontinuity every second interface.

Since our goal is to keep the energy as confined as pos-

sible in the vacuum inner layer, i.e., maximal interaction impedance, we may choose one of the dielectric materials to have  $\epsilon = 2$ , and the other dielectric as large as possible. This will indeed create maximum attenuation per unit cell, however the interaction impedance depends on the total flowing power outside the vacuum layer, which tends to grow when low dielectric coefficient materials are used and the layers become thicker. Consequently, there exists a tradeoff between creating high contrast between the two materials, and using low dielectric coefficient materials. For instance, choosing one dielectric material to have  $\epsilon = 2$  and the other as small as possible would result in high attenuation per period, but very low interaction impedance.

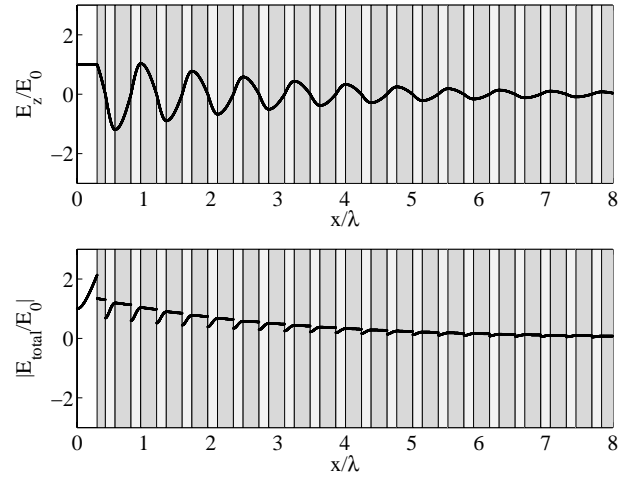


Figure 2: A typical distribution of the longitudinal electric field and the total electric field ( $D_{\text{int}} = 0.3\lambda$ ,  $\epsilon^{\text{I}} = 2.1$ ,  $\epsilon^{\text{II}} = 4$ ).

## 4 ACCELERATOR PARAMETERS

### 4.1 Interaction Impedance

The interaction impedance is a measure of the accelerating gradient experienced by the electrons for a given amount of power injected into the system. Denoting by  $P$  the flowing power per unit length of  $y$ , the interaction impedance per unit length is defined by  $Z_{\text{int}}[\Omega m] \triangleq |\lambda E_0|^2 / P$ . Assuming that the materials' characteristics are known ( $\epsilon^{\text{I}} = 2.1, \epsilon^{\text{II}} = 4$ ) and so is the laser wavelength ( $\lambda$ ), the only free parameter left is the width of the internal vacuum layer  $2D_{\text{int}}$ . Based on simulations, it was found that for  $0.3 \leq D_{\text{int}}/\lambda \leq 0.8$ , the best fit for the interaction impedance is given by

$$\begin{aligned} \frac{Z_{\text{int}}}{\eta_0 \lambda} (\epsilon^{\text{I}} = 2.1, \epsilon^{\text{II}} = 4) \simeq & 1.124 - 3.561 \frac{D_{\text{int}}}{\lambda} \\ & + 4.258 \left( \frac{D_{\text{int}}}{\lambda} \right)^2 - 1.823 \left( \frac{D_{\text{int}}}{\lambda} \right)^3 \end{aligned} \quad (5)$$

which means  $Z_{\text{int}}/\lambda$  decreases monotonically from about  $147\Omega$  to about  $26\Omega$ .

Holding the vacuum region width to a constant value ( $D_{\text{int}} = 0.3\lambda$ ), Fig. 3 shows the contours of constant interaction impedance as a function of  $(\epsilon^{\text{I}}, \epsilon^{\text{II}})$ . Since no confinement is expected when the medium is uniform ( $\epsilon^{\text{I}} = \epsilon^{\text{II}}$ ), the interaction impedance is virtually zero on the diagonal. Similarly, when either one of the dielectric coefficients is close to unity, the thickness of the layer being proportional to  $1/\sqrt{\epsilon - 1}$  implies large confinement space and therefore, low interaction impedance. In between these three minima regions there are two *asymmetric* regions of maximum interaction impedance. The asymmetry is dictated by the choice of the dielectric consisting the first layer ( $\epsilon^{\text{I}}$ ). For the vacuum layer width chosen here, a larger impedance is obtained when the first layer is of lower value, but this trend may change for a different value of  $D_{\text{int}}$ . Clearly, a *high dielectric coefficient* can significantly increase the interaction impedance. For example, taking Silica for the first layer and a material with  $\epsilon = 25$  for the second layer, leads to an interaction impedance per wavelength of  $471\Omega$ .

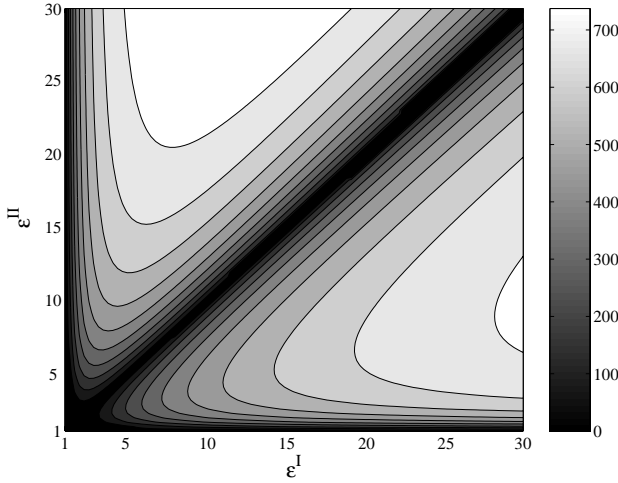


Figure 3: Contours of constant interaction impedance  $Z_{\text{int}}/\lambda[\Omega]$  as a function of  $(\epsilon^{\text{I}}, \epsilon^{\text{II}})$ , with  $D_{\text{int}} = 0.3\lambda$ .

## 4.2 Energy Velocity

Denoting the energy density by  $w_{\text{EN}}$ , we define the average energy per unit length as  $W \triangleq \int_{-\infty}^{\infty} dx w_{\text{EN}}(x)$  and the energy velocity is defined by  $v_{\text{EN}}/c \triangleq P/(cW)$ . According to our simulations, for  $0.3 \leq D_{\text{int}}/\lambda \leq 0.8$ , the energy velocity increases monotonically from about  $0.42c$  to about  $0.53c$ . As before, the best fit of the simulation results is given by

$$\frac{v_{\text{EN}}}{c}(\epsilon^{\text{I}} = 2.1, \epsilon^{\text{II}} = 4) \simeq 0.342 + 0.290 \left( \frac{D_{\text{int}}}{\lambda} \right) - 0.061 \left( \frac{D_{\text{int}}}{\lambda} \right)^2 \quad (6)$$

## 4.3 Maximum Electric Field

The last parameter of interest is the maximum electric field sustained by the structure before breakdown. According to (1) the magnitude of the electric field vector increases from a local minimum on axis, to a larger value

$$\frac{E_{\text{max}}}{E_0} = \sqrt{1 + \left( \frac{2\pi D_{\text{int}}}{\lambda} \right)^2} \quad (7)$$

at the vacuum-dielectric discontinuity; for most practical purposes this may also be considered the maximum electric field – fact revealed also by the bottom frame of Fig. 2. For avoiding breakdown it is assumed that the fluence threshold of the material limits the maximum field to about  $2\text{GV/m}$ . Therefore, bearing in mind that the gradient of interest is of the order  $1\text{GV/m}$ , then Eq. (7) entails the inner layer half-width should be

$$\frac{E_{\text{max}}}{E_0} = 2 \Rightarrow D_{\text{int}} \simeq 0.28\lambda \quad (8)$$

## 5 CONCLUSION

In the present study we have designed and analyzed an accelerator based on a Bragg reflection waveguide, where the layers have a width of a quarter of the transverse propagation wavelength  $\lambda/(4\sqrt{\epsilon - 1})$ . An interaction impedance per wavelength of over  $100\Omega$  is feasible with existing materials. Materials of high dielectric coefficient can significantly improve the interaction impedance per wavelength to hundreds of Ohms.

The planar structure provides a good analogy, especially asymptotically, to a hollow *cylindrical* Bragg fiber accelerator. A cylindrical structure would have a higher interaction impedance than a planar structure for an internal radius  $R_{\text{int}} = D_{\text{int}}$  for two reasons. For a given gradient the *maximum* field would be smaller as the radial electric field  $E_r = \frac{j}{2} \frac{\omega}{c} r E_0 e^{-j \frac{\omega}{c} z}$  would be smaller by a factor of 2. The second reason is that in addition to the radial exponential decay, in the cylindrical case there would be a  $1/r$  decay due to the cylindrical wave functions.

## 6 REFERENCES

- [1] Y. C. Huang, D. Zheng, W. M. Tulloch, and R. L. Byer, “Proposed structure for a crossed-laser beam, GeV per meter gradient, vacuum electron linear accelerator,” *Applied Physics Letters*, vol. 68, pp. 753–755, February 1996.
- [2] J. D. Lawson, “Lasers and accelerators,” *IEEE Transactions on Nuclear Science*, vol. 26, pp. 4217–19, June 1979.
- [3] P. M. Woodward, *J. IEE*, vol. 93, p. 1554, 1947.
- [4] X. E. Lin, “Photonic band gap fiber accelerator,” *Physical Review Special Topics – Accelerators and Beams*, vol. 4, pp. 051301 1–7, May 2001.
- [5] P. Yeh and A. Yariv, “Bragg reflection waveguides,” *Optics Communications*, vol. 19, pp. 427–430, December 1976.